PERGAMON

International Journal of Solids and Structures 36 (1999) 1105–1128

INTERNATIONAL JOURNAL OF SOLIDS and STRUCTURES

3-D elastic stress singularity at polyhedral corner points

Evgeny Glushkov,* Natalya Glushkova, Olga Lapina

Kuban State University, P.O. Box 4102, Krasnodar 350080, Russia

Received 22 December 1996

Abstract

The three-dimensional stress singularity at the top of an arbitrary polyhedral corner is considered. Based on the boundary integral equations, the problem is reduced by the Mellin transform to a system of certain one-dimensional integral equations. The orders of stress singularity are spectral points of the integral operators while angular distribution and intensity factors are found as residues at those points. Numerical results are obtained by means of the Galerkin discretization scheme using expansions in terms of orthogonal polynomials with the proper weights. Some of the results illustrating the order's dependence on the elastic properties and corner geometry for a wedge-shaped punch and a crack, for an elastic trihedron and for a surface-breaking crack are given.

1. Introduction

In two-dimensional (2D) elasticity, a stress field near a corner point is of the form

$$\tau \sim \Sigma \mathbf{c}_i(\varphi) r^{-\gamma_i}, \quad 1 > Re\,\gamma_1 > Re\,\gamma_2 > \cdots > Re\,\gamma_n > \cdots, \quad r \to 0$$

where (r, φ) are the polar co-ordinates centred at the vertex and $\mathbf{c}_i(\varphi)$ are smooth functions. This form was obtained and investigated by Williams (1952), Karp and Karal (1962), Bogy (1968), England (1971), and Theocaris (1974) among others. Power exponents γ_i depend on the angle opening, in particular, when the corner degenerates into a thin slit, there is well-known value $\gamma_1 = 0.5$.

But in three space variables the situation is not resolved so easily. For example, when the crack contour has a corner point, the stress field in its vicinity is essentially three-dimensional (3-D) [it is a so-called singularity of "conical type" (Kondrat'ev, 1968; Bazant, 1974) or a "3-D singularity"] and the results above become inapplicable. In the case of an arbitrary polyhedral corner the exponents cannot be found as the roots of algebraic eigenequations, they are the spectral points of

* Corresponding author. E-mail: evg@kgu.kuban.su.

0020–7683/99/$ - see front matter
PII: S0020–7683(97)00361–2

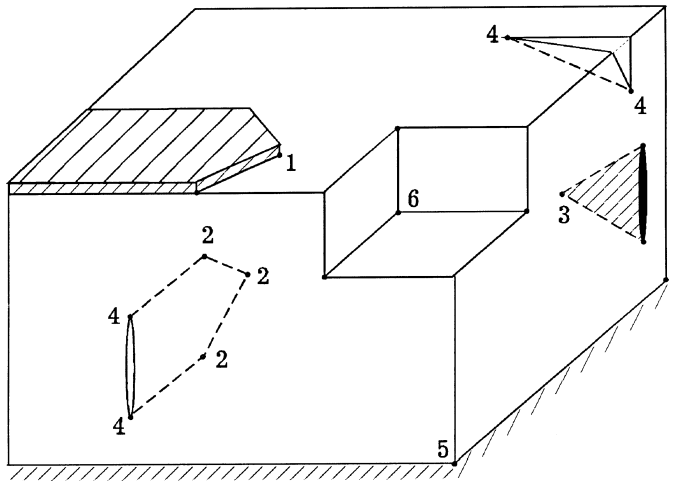

Fig. 1. Examples of the 3-D singular points: wedge-shaped punch, crack, and inclusion (1–3), surface-breaking cracks (4), top of a cube (5), brick-out corner (6).

the boundary value problems reduced to boundary integral equations (BIEs) or certain variational eigenproblems. Several examples of possible 3-D singularity points are given in Fig. 1.

Depending on the number of variables to be discretised the methods of 3-D singularity extracting can be subdivided into three groups:

(1) a direct volume discretisation (3-D FEM);
(2) a separating out the $r^{-\gamma}$ factor analytically and discretisation with respect to two spherical angular variables;
(3) an application of the Mellin transform to the BIEs and discretisation with respect to only angular polar variable connected with the wedge-shaped sides of a polyhedral vertex.

The first way is not too complicated analytically but leads to algebraic systems of about 10–20 thousand equations [for example, 11,000 equations in the crack-surface intersection problem considered by Becker and Schnack (1990)], i.e. it required the use of supercomputers. In the second case, from 500 (Abdei-Messiei and Thatcher, 1990; Ghahremani, 1991; Leguillon, 1995) to 2400 (Matveenko and Minakova, 1988) equations are dealt with and workstations are employed as usual. We have been developing the third approach (Babeshko et al., 1981, 1989, 1991; Glushkov and Glushkova, 1988, 1992; Lapina, 1992; Glushkov et al., 1996), which involves rather complicated prior analytical calculations, but systems of about 10–30 equations are solved with personal computers to obtain the same accuracy as above.

The first goal of the present paper is to give a general idea of the method and a review of the numerical results obtained earlier for wedge-shaped punches and cracks, and secondly, to give the recent results for the top of an elastic trihedron with one fixed side and for a surface-breaking crack.

2. General scheme

2.1. *Wiener–Hopf type integral equations*

Among the variety of 3-D singularity problems there is a common special case when a polyhedral elastic volume is unfolded completely in a space or in a half-space so that all its sides lie in a plane. For instance, there are a wedge-shaped punch contacting with a half-space, a wedge-shaped planar crack or an inclusion (points 1–3 in Fig. 1), including the interface ones located between two dissimilar materials. Those problems are reduced to the Wiener–Hopf type integral equation in the wedge-shaped area Ω: $0 \leqslant r \leqslant \infty$, $-\theta \leqslant \varphi \leqslant \theta$ (Fig. 2):

$$\int\int_{\Omega} \mathbf{k}(x-\xi, y-\eta)\mathbf{q}(\xi,\eta)\,\mathrm{d}\xi\,\mathrm{d}\eta = \mathbf{f}(x,y), \quad (x,y)\in\Omega \tag{1}$$

$$\mathbf{k}(x,y) = \frac{1}{4\pi^2}\int\int_{-\infty}^{\infty} \mathbf{K}(\alpha_1,\alpha_2)e^{-i(\alpha_1 x+\alpha_2 y)}\,\mathrm{d}\alpha_1\,\mathrm{d}\alpha_2 \tag{2}$$

$$\begin{cases} x = r\cos\varphi \\ y = r\sin\varphi \\ r = \sqrt{x^2+y^2} \end{cases} \quad \begin{cases} \xi = \rho\cos\psi \\ \eta = \rho\sin\psi \\ \rho = \sqrt{\xi^2+\eta^2} \end{cases} \quad \begin{cases} \alpha_1 = \alpha\cos\beta \\ \alpha_2 = \alpha\sin\beta \\ \alpha = \sqrt{\alpha_1^2+\alpha_2^2} \end{cases} \tag{3}$$

with a homogeneous Fourier symbol of the matrix-kernel $\mathbf{k}$: $\mathbf{K}(t\alpha_1, t\alpha_2) = t^p\mathbf{K}(\alpha_1,\alpha_2)$ or equivalently $\mathbf{K}(\alpha_1,\alpha_2) = \alpha^p\mathbf{\Phi}(\beta)$ [see below eqn (16) with $z = 0$ for a punch and eqn (34) for a crack as examples of $\mathbf{K}$].

From here on we shall use capital letters with arguments α_1, α_2 to denote the Fourier transforms with respect to x, y:

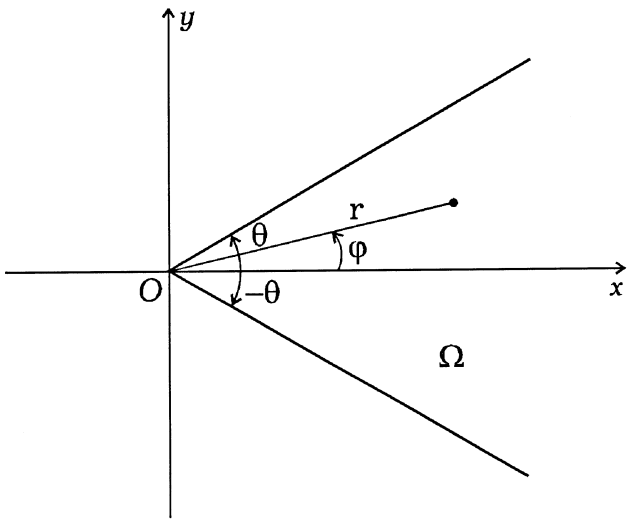

Fig. 2. Wedge-shaped area Ω and polar co-ordinates.

$$\mathbf{K}(\alpha_1, \alpha_2) = \int\int_{-\infty}^{\infty} \mathbf{k}(x, y) e^{i(\alpha_1 x + \alpha_2 y)} \, \mathrm{d}x \, \mathrm{d}y,$$

$$\mathbf{Q}(\alpha_1, \alpha_2) = \int\int_{\Omega} \mathbf{q}(x, y) e^{i(\alpha_1 x + \alpha_2 y)} \, \mathrm{d}x \, \mathrm{d}y, \quad \text{etc.}$$

whereas the Mellin transforms

$$\mathbf{Q}(s, \varphi) = M_s[\mathbf{q}] \equiv \int_0^{\infty} \mathbf{q}(r, \varphi) r^{s-1} \, \mathrm{d}r,$$

$$\mathbf{q}(r, \varphi) = M_s^{-1}[\mathbf{Q}] \equiv \frac{1}{2\pi i} \int_{c-i\infty}^{c+i\infty} \mathbf{Q}(s, \varphi) r^{-s} \, \mathrm{d}s$$

will be distinguished by dependence of parameter s and angular variables.

The Mellin transform M_s, being applied to eqn (1) with respect to parameter r, converts it, owing to the homogeneity, into a one-fold integral equation relative to the Mellin transform of $\mathbf{q}$:

$$\int_{-\theta}^{\theta} \mathbf{K}(s, \varphi - \psi) \mathbf{Q}(s - p, \psi) \, \mathrm{d}\psi = \mathbf{F}(s, \varphi), \quad -\theta \leqslant \varphi \leqslant \theta \tag{4}$$

where

$$\mathbf{K}(s, \varphi - \psi) = M_s[\mathbf{k}] \rho^{-(s-p-2)}$$

$$\mathbf{Q}(s - p, \psi) = M_{s-p}[\mathbf{q}] \equiv \int_0^{\infty} \mathbf{q}(\rho, \psi) \rho^{s-p-2} \rho \, \mathrm{d}\rho.$$

As is generally known from complex analysis, an expansion of a function at the point $r = 0$:

$$f(r, \varphi) \sim \sum_i c_i(\varphi) r^{-\gamma_i}, \quad r \to 0$$

is determined by the analytical properties of its Mellin transform $F(s, \varphi)$. Namely, $\gamma_i = s_i$ are the poles of $F(s, \varphi)$ and $c_i = \operatorname{res} F(s, \varphi)|_{s=s_i}$. Thus, to obtain power exponents γ_i for the $\mathbf{q}(r, \varphi)$ expansion as $r \to 0$, one can find the poles of $\mathbf{Q}(s, \varphi)$, i.e. the spectral points of integral operator eqn (4) in the complex s-plane.

Equation (4) is discretised in line with Galerkin's method or collocation scheme. Substitution of an expansion of $\mathbf{Q}(s - p, \psi)$ in terms of certain basis functions $v_k(\psi)$:

$$\mathbf{Q}(s - p, \psi) = \sum_{k=0}^{\infty} \mathbf{t}_k(s) v_k(\psi) \tag{5}$$

into the integral equation and projection of the discrepancy upon the second basis $\{w_l(\varphi)\}_{l=1}^{\infty}$ leads to an infinite algebraic system:

$$\mathbf{A}(s)\mathbf{t}(s) = \mathbf{f}(s)$$

$$\mathbf{A} = \|\mathbf{a}_{lk}\|_{lk=0}^{\infty}, \quad \mathbf{t} = (\mathbf{t}_0, \mathbf{t}_1, \mathbf{t}_2, \ldots), \quad \mathbf{f} = (\mathbf{f}_0, \mathbf{f}_1, \mathbf{f}_2, \ldots)$$

$$\mathbf{a}_{lk} = \int\int_{-\theta}^{\theta} \mathbf{K}(s, \varphi-\psi) v_k(\psi) w_l(\varphi)\, \mathrm{d}\psi\, \mathrm{d}\varphi$$

$$\mathbf{f}_l = \int_{-\theta}^{\theta} \mathbf{f}(\varphi) w_l(\varphi)\, \mathrm{d}\varphi. \tag{6}$$

The spectral points s_i coincide with zeros of the determinant:

$$s_i: \quad \Delta(s_i) \equiv \det \mathbf{A}(s)\,|_{s=s_i} = 0. \tag{7}$$

With the shift $s-p$ at the first variable of $\mathbf{Q}$ the desired orders $\gamma_i = s_i - p$.

As usual, the expansion of function $\mathbf{q}$ itself is not so important for practical purposes, however, the required singular terms of the stress–strain field as $r \to 0$ can be expressed explicitly as residuals basing upon the corresponding integral representations of the field in terms of $\mathbf{q}$ or other auxiliary functions [see below eqns (27), (38) and (43) as examples of the field expansion]. The stress orders γ_i with $Re\ \gamma_i > 3/2$ ($Re\ \gamma_i = 3/2$ if $\mathrm{Im}\ \gamma_i = 0$) are impermissible because such stress terms $c_i r^{-\gamma_i}$ yield an infinite strain-energy in the vertex vicinity (in the 2D case this occurs with $Re\ \gamma_i > 1$). Note, that to take into account the contribution of all permissible poles and to cut off the impermissible ones, the integration path of the inverse Mellin transform M_s^{-1} must go vertically at the right side of the strip of singularity, leaving the permissible poles at the left and impermissible ones at the right hand sides of the path.

An important property making the scheme practically executable and efficient is a series representation of the kernel with separated out angular variables. For its derivation consider $\mathbf{k}$ in polar co-ordinates (eqn (3)):

$$\mathbf{k}(x-\xi, y-\eta) = \frac{1}{4\pi^2} \int_0^{\infty} \alpha^{p+1} \int_0^{2\pi} \mathbf{\Phi}(\beta) e^{-i\alpha r\cos(\varphi-\beta)} e^{i\alpha\rho\cos(\psi-\beta)}\, \mathrm{d}\beta\, \mathrm{d}\alpha. \tag{8}$$

For an isotropic elastic material elements of the matrix $\mathbf{K}(\alpha_1, \alpha_2)$ depend on cofactors $\alpha_1^{p_1}\alpha_2^{p_2}\alpha^{p_3}$, $p_1+p_2+p_3 = p$ with integer exponents p_i only. Hence, $\mathbf{\Phi}(\beta)$, depending on $\cos^{p_1}\beta \sin^{p_2}\beta$, is a finite linear combination of the exponents $e^{in\beta}$, so that the elements of the kernel $\mathbf{k}$ may be expressed as the linear combination of the integrals

$$I_n = \frac{1}{4\pi^2} \int_0^{\infty} \alpha^{p+1} \int_0^{2\pi} e^{in\beta} e^{-i\alpha r\cos(\varphi-\beta)} e^{i\alpha\rho\cos(\psi-\beta)}\, \mathrm{d}\beta\, \mathrm{d}\alpha, \quad n = 0, \pm 1, \pm 2, \ldots, \pm M. \tag{9}$$

Namely, factor α_1 in $\mathbf{K}(\alpha_1, \alpha_2)$ is replaced by $(I_1+I_{-1})/2$, α_1^2 by $(I_2+2I_0+I_{-2})/4$, $\alpha_1\alpha_2$ by $(I_2-I_{-2})/4i$ and so forth.

Integrals in eqn (9), in turn, are reduced to the following series:

$$I_n = \frac{i^n}{2\pi} e^{in\psi} \sum_{m=-\infty}^{\infty} \int_0^{\infty} J_m(\alpha r) J_{m+n}(\alpha\rho) \alpha^{p+1}\, \mathrm{d}\alpha\, e^{-im(\varphi-\psi)} \tag{10}$$

which has been derived using the equality (Bateman and Erdélyi, 1953):

$$e^{it\sin\varphi} = \sum_{m=-\infty}^{\infty} J_m(t)e^{im\varphi}$$

($J_v(z)$ is the Bessel function).

For an anisotropic material, elements of $\mathbf{\Phi}(\beta)$ in eqn (8) are smooth functions of β that also can be expanded in terms of $e^{in\beta}$ in a Fourier series. Though in the general case the series are infinite, by virtue of smoothness they are fast-convergent and can be effectively truncated so that the kernel is expressed in terms of a finite number of the integrals I_n too. As an example, such an approach has been used in the problem for a wedge-shaped punch moving across the surface of an elastic half-space with sliding friction (Glushkov and Glushkova, 1988; Babeshko et al., 1989). The motion leads to an anisotropy of the wave speeds in the local moving co-ordinates.

Hypersingularity of the kernel $\mathbf{k}$ is reflected in the divergence of integrals (9) and series (10) in a classical sense. However, since $\mathbf{k}$ is an integrand, all operations with such representations carried out in the framework of the scheme described, including application of the Mellin transform, are strictly justified similarly as the use of the generalised functions (Schwartz, 1950–1951) (in fact, $\mathbf{K}(\alpha_1, \alpha_2)$ is a matrix-symbol of a pseudodifferential operator (Taylor, 1981)).

Based upon the equality (Ditkin and Prudnikov, 1974)

$$M_s[J_m(\alpha r)] = \alpha^{-s}2^{s-1}\Gamma\left(\frac{m+s}{2}\right)\Big/\Gamma\left(\frac{m-s+2}{2}\right)$$

one can derive from eqn (10)

$$M_s[I_n] = \rho^{s-p-2}\frac{i^n e^{in\psi}}{2\pi}\sum_{m=-\infty}^{\infty} g_m(s,n)e^{-im(\varphi-\psi)} \tag{11}$$

$$g_m(s,n) = G_1(s,m)G_2(s,m+n) \sim O(m^p), \quad m \to \infty$$

$$G_1(s,m) = \Gamma\left(\frac{m+s}{2}\right)\Big/\Gamma\left(\frac{m-s+2}{2}\right),$$

$$G_2(s,m) = 2^p\Gamma\left(\frac{m-s+2+p}{2}\right)\Big/\Gamma\left(\frac{m+s-p}{2}\right).$$

By this means the application of the Mellin transform to eqn (1) leads to one-fold eqn (4) with the kernel $\mathbf{K}$ expressed as the linear combination of series eqn (11) (without the factor ρ^{s-p-2} entered in $\mathbf{Q}(s-p,\psi)$), and thereby after discretisation, elements $\mathbf{a}_{lk}$ of system (6) may be represented in closed algebraic (computable) form in terms of series

$$\hat{I}_n = \frac{i^n}{2\pi}\left[\frac{1}{2}i_0(s,n) + \sum_{m=1}^{\infty} i_m(s,n)\right] \tag{12}$$

where

$$i_m(s,n) = g_m(s,n)\,d_m(n) + (-1)^n g_m(s,-n) d_m^*(-n)$$

$$\times d_m(n) = d_1(m+n,k) d_2(m,l) \begin{cases} d_1(m,k) = \int_{-1}^{1} v_k(\psi) e^{im\psi}\,\mathrm{d}\bar{\psi}, & \bar{\psi} = \psi/\theta \\ d_2(m,l) = \int_{-1}^{1} w_l(\varphi) e^{im\varphi}\,\mathrm{d}\bar{\varphi}, & \bar{\varphi} = \varphi/\theta \end{cases} . \tag{13}$$

An asterisk at d_m^* denotes the complex-conjugate value. Note that for obtaining $\mathbf{a}_{lk}$, it is enough to replace I_n by $\hat{I}_n$ in the kernel structure.

It should be pointed out that series (12) is already convergent despite the divergence of initial series (10). The convergence is ensured by the required decrease of the d_m factors. Their behaviour as $m \to \infty$ may be found as a contribution of the limit points $\bar{\varphi}$, $\bar{\psi} = \pm 1$ in the asymptotics of oscillate integrals (13). The latter is dictated by the behaviour of the basis functions at the limit points, i.e. it depends on the proper choice of orthogonal polynomials as $v_k(\psi)$ and $w_l(\varphi)$. In the general case they are Jacobi polynomials:

$$v_k(\psi) = (1-\bar{\psi})^{\delta_1}(1+\bar{\psi})^{\delta_2} P_k^{(\delta_1,\delta_2)}(\bar{\psi}) \tag{14}$$

with the weight $(1-\bar{\psi})^{\delta_1}(1+\bar{\psi})^{\delta_2}$ describing the required behaviour of the unknown $\mathbf{q}(\rho,\psi)$ at the edges $\psi/\theta = \pm 1$, such as the square-root behaviour $(\theta^2-\psi^2)^{1/2}$ of the crack opening displacement (c.o.d.) for a wedge-shaped crack or the square-root singularity $(\theta^2-\psi^2)^{-1/2}$ of the contact stress for a punch. This behaviour has to be found *a priori* from the corresponding 2D problems for dihedral corners (elastic wedges).

As an illustration, in the simplest case of a wedge-shaped crack, mode I, integral eqn (1) is scalar with $K(\alpha_1,\alpha_2) = c\alpha$ ($p = 1$). Unknown $q(\rho,\psi)$ in this case is the normal component of the c.o.d. Therefore, one must take $\delta_1 = \delta_2 = 1/2$ in eqn (14), i.e. Chebyshev polynomials of the second kind as $v_k(\psi)$. As for projectors $w_l(\psi)$, the Legendre polynomials $P_l(\bar{\psi})$ ($\delta_1 = \delta_2 = 0$) are quite acceptable, because the discrepancy expanded in terms of w_l is a smooth function. Such a choice in this example assures decrease $i_m \sim O(m^{-3/2})$ as $m \to \infty$.

Note, that although expansion in Fourier series ($v_k(\psi) = e^{ik\pi\bar{\psi}}$) or in Legendre polynomials $P_k(\bar{\psi})$ seems to be natural, it would give $i_m \sim O(m^{-1})$, as $m \to \infty$, i.e. divergent series in the final expressions for computing. And conversely, the divergence in the final representations indicates a non-acceptable basis with incorrect behaviour at the edges. Of even greater interest is the fact that those basis functions also did not assure numerical stability of the results in the punch problem, though the convergence was even faster than with the orders $\delta_1 = \delta_2 = -1/2$ required here. Hence, the numerical stability may serve as an experimental criterion for the proper choice of the weight if there is not any other information on the behaviour of the unknown function at the limit points (as an example, at the line of the crack-surface intersection in Section 4.2).

Convergence as $O(m^{-3/2})$ is rather slow for efficient computation, therefore we accelerate the series by extracting several terms of $i_m(s,n)$ asymptotics as $m \to \infty$ analytically and summing up them explicitly with help of representations like (Ditkin and Prudnikov, 1974)

$$\sum_{m=1}^{\infty} \frac{e^{im\theta}}{m^{\nu}} = \frac{1}{\Gamma(\nu)} \int_0^{\infty} \frac{t^{\nu-1}(e^{i\theta}-e^{-t})e^{-t}\,\mathrm{d}t}{1-2e^{-t}\cos\theta+e^{-2t}}.$$

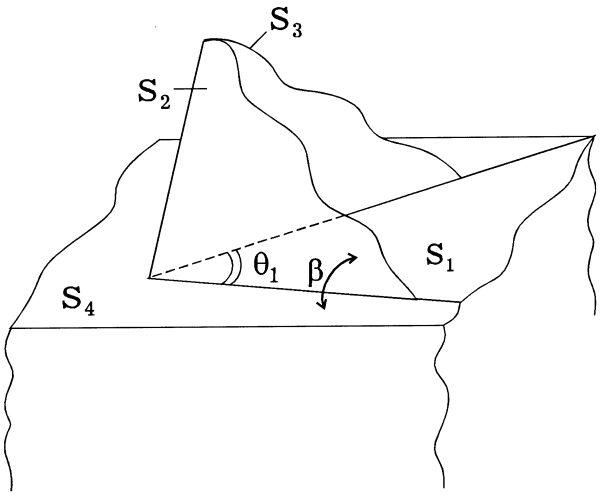

Fig. 3. Trihedral elastic volume stuck to a half-space.

2.2. *General case*

The scheme described above remains valid in the general case when the sides do not lie in a plane, for example, as is shown in Fig. 3, but, naturally, its realisation is a more challenging problem in this case, because, instead of Wiener–Hopf eqn (1), the BIEs have to be dealt with. Usually the BIEs are derived from the volume integrals in accordance with the divergence theorem. Those equations may be used in the context of this scheme too, however, with the polyhedral volumes considered, it seemed to be more convenient to employ integral equations derived as superposition of displacement and stress fields $\mathbf{u}^{ij}$, τ^{ij} caused by surface loads $\mathbf{q}_j$ in the elastic half-spaces which surfaces coincide with the sides S_j of the polyhedron:

$$\mathbf{u}^{ij}(\mathbf{x}_j) = \mathscr{K}^{ij}\mathbf{q}_j \equiv \frac{1}{4\pi^2}\mathbf{P}_{ij}\int\int_{-\infty}^{\infty}\mathbf{K}(\alpha_1,\alpha_2,z_j)\mathbf{Q}_j(\alpha_1,\alpha_2)e^{-i(\alpha_1 x_j+\alpha_2 y_j)}\,\mathrm{d}\alpha_1\,\mathrm{d}\alpha_2,$$

$$\tau^{ij}(\mathbf{x}_j) = \mathscr{T}^{ij}\mathbf{q}_j \equiv \frac{1}{4\pi^2}\mathbf{P}_{ij}\int\int_{-\infty}^{\infty}\mathbf{T}^{ij}(\alpha_1,\alpha_2,z_j)\mathbf{Q}_j(\alpha_1,\alpha_2)e^{-i(\alpha_1 x_j+\alpha_2 y_j)}\,\mathrm{d}\alpha_1\,\mathrm{d}\alpha_2. \tag{15}$$

Here $\mathbf{x}_j = (x_j, y_j, z_j) \in S_i$ is a point of the j-th half-space $z_j \leqslant 0$, $-\infty \leqslant x_j, y_j \leqslant \infty$ in the Cartesian co-ordinates centred at the vertex, plane $z_j = 0$ coincides with S_j (Fig. 4), $\mathbf{u}^{ij}$, τ^{ij} are in the coordinate systems connected with S_i, $\mathbf{P}_{ij}$ are conversion matrices from $\mathbf{x}_j$ to $\mathbf{x}_i$ co-ordinates,

$$\mathbf{K}(\alpha_1,\alpha_2,z) = \begin{pmatrix} \alpha_1^2\alpha z - 2\nu\alpha_1^2 + 2\alpha^2 & \alpha_1\alpha_2(\alpha z - 2\nu) & i\alpha_1\alpha(\alpha z + \nu_1) \\ \alpha_1\alpha_2(\alpha z - 2\nu) & \alpha_2^2\alpha z - 2\nu\alpha_2^2 + 2\alpha^2 & i\alpha_2\alpha(\alpha z + \nu_1) \\ i\alpha_1\alpha(\alpha z - \nu_1) & i\alpha_2\alpha(\alpha z - \nu_1) & -\alpha^2(\alpha z - \nu_2) \end{pmatrix}\frac{e^{\alpha z}}{2\alpha^3\mu} \tag{16}$$

$$\nu_1 = 1-2\nu, \quad \nu_2 = 2(1-\nu)$$

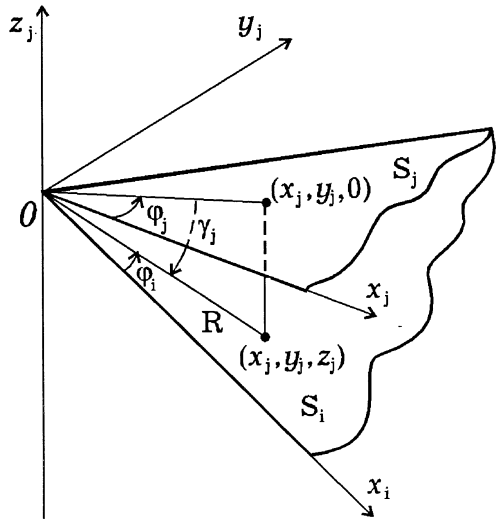

Fig. 4. Some sides S_i and S_j of a polyhedron. Connected with S_j spherical co-ordinates φ_j, γ_j of a point lying on S_i are determined uniquely as functions of $\varphi_i \in S_i$.

$$\mathbf{T}^{ij}(\alpha_1, \alpha_2, z) = (\mathbf{M}_1\mathbf{n}_j^i | \mathbf{M}_2\mathbf{n}_j^i | \mathbf{M}_3\mathbf{n}_j^i), \tag{17}$$

where $\mathbf{n}_j^i$ are the outward unit normals to S_i in the $\mathbf{x}_j$ co-ordinates,

$$\mathbf{M}_j = \begin{pmatrix} s_{2j} & s_{1j} & r_{1j} \\ s_{1j} & s_{3j} & r_{2j} \\ r_{1j} & r_{2j} & r_{3j} \end{pmatrix}, \quad j = 1, 2, 3$$

s_{mn}, r_{mn} are components of the matrices

$$\mathbf{S} = -\begin{pmatrix} \alpha_2(\alpha_2^2 + \alpha_1^2 b) & \alpha_1(\alpha_1^2 + \alpha_2^2 b) & i\alpha_1\alpha_2\alpha b \\ \alpha_1(\alpha_1^2\alpha z + c_2) & \alpha_2(\alpha_1^2\alpha z + 2\nu\alpha_2^2) & i(\alpha_1^2\alpha b + 2\nu\alpha^3) \\ \alpha_1(\alpha_2^2\alpha z + 2\nu\alpha_1^2) & \alpha_2(\alpha_2^2\alpha z + c_1) & i(\alpha_2^2\alpha b + 2\nu\alpha^3) \end{pmatrix} \frac{ie^{\alpha z}}{\alpha^3}$$

$$b = \alpha z + \nu_1, \quad c_k = 2(\alpha^2 + \nu\alpha_k^2), \quad k = 1, 2$$

$$\mathbf{R} = \begin{pmatrix} \alpha_1^2 z + \alpha & \alpha_2\alpha_2 z & i\alpha_1\alpha z \\ \alpha_1\alpha_2 z & \alpha_2^2 z + \alpha & i\alpha_2\alpha z \\ i\alpha_1\alpha z & i\alpha_2\alpha z & \alpha - \alpha^2 z \end{pmatrix} \frac{e^{\alpha z}}{\alpha},$$

ν is the Poisson ratio and μ is the shear module of the elastic material.

Reasoning from eqn (15), the displacement and stress fields in a convex polyhedral elastic volume V are expressed in the $\mathbf{x}_i$ co-ordinate system as

$$\begin{cases} \mathbf{u}^i(\mathbf{x}) = \sum_j \mathscr{K}^{ij}\mathbf{q}_j, \\ \tau^i(\mathbf{x}) = \sum_j \mathscr{T}^{ij}\mathbf{q}_j \end{cases} \quad \mathbf{x} \in V. \tag{18}$$

As an example, in the case of a trihedral corner with a given boundary displacement $\mathbf{v}_1$ at the side S_1 and loads $\mathbf{p}_2$, $\mathbf{p}_3$ at the sides S_2, S_3 (Fig. 3, point 5 in Fig. 1) the superposition yields the following BIEs:

$$\begin{cases} \sum_{j=1}^{3} \mathscr{K}^{1j}\mathbf{q}_j = \mathbf{v}_1, \quad \mathbf{x} \in S_1 \\ \sum_{j=1}^{3} \mathscr{T}^{ij}\mathbf{q}_j = \mathbf{p}_i, \quad \mathbf{x} \in S_i, \quad i = 2, 3. \end{cases} \tag{19}$$

Though this representation is valid for a convex polyhedron only (its volume must belong to all half-spaces) such a technique is quite applicable to a non-convex volume as well, if it is divided into convex parts and the sewing conditions between them are added. Thus, if it is supposed that the trihedron considered is stuck to an elastic base, we have to add to eqn (19) the equality for the fourth underlying half-space $z_4 \leqslant 0$ (Fig. 3):

$$\mathbf{v}_4 = \mathscr{K}^{44}\mathbf{q}_4, \quad \mathbf{x} \in S_4 \tag{20}$$

and the sewing conditions:

$$\begin{cases} \mathbf{v}_1 = \mathbf{P}_{14}\mathbf{v}_4 \\ \mathbf{q}_1 = \mathbf{P}_{14}\mathbf{q}_4 \end{cases}, \quad \mathbf{x} \in S_1 \subset S_4 \tag{21}$$

($\mathbf{v}_1$ is the unknown here).

Since the radial distance $R = \sqrt{x_j^2 + y_j^2 + z_j^2}$ is the same with any co-ordinate system $\mathbf{x}_j$ centred at the top, the Mellin transform is also applicable to BIEs (19)–(21). In addition to greater complexity of these equations in comparison with eqn (1), the main qualitative distinction is that the kernel symbols of the $\mathscr{K}^{ij}$, $\mathscr{T}^{ij}$ operators contain an extra factor $e^{\alpha z_j}$, so that the kernels are represented in terms of integrals

$$\frac{1}{4\pi^2}\int_{-\infty}^{\infty}\int_{-\infty}^{\infty} \alpha_1^{p_1}\alpha_2^{p_2}\alpha^{p_3}e^{\alpha z}e^{-i(\alpha_1(x-\xi)+\alpha_2(y-\eta))}\,\mathrm{d}\alpha_1\,\mathrm{d}\alpha_2, \quad z \leqslant 0. \tag{22}$$

This factor $e^{\alpha z}$, connected with transmission of a surface loading into a depth of a half-space, complicates the use of the Mellin transform and discretisation. The basic integrals I_n for eqn (22) [analogue of integrals (9) and (10)] take in spherical co-ordinates

$$\begin{cases} x = R\cos\gamma\cos\varphi, & R = \sqrt{x^2+y^2+z^2} \\ y = R\cos\gamma\sin\varphi, & r = \sqrt{x^2+y^2} = R\cos\gamma \\ z = R\sin\gamma, & -\pi/2 \leqslant \gamma \leqslant 0 \end{cases}$$

the following form:

$$I_n(\gamma) = \frac{1}{4\pi^2}\int_0^\infty \alpha^{p+1}\int_0^{2\pi} e^{in\beta}e^{-i\alpha R\cos\gamma\cos(\varphi-\beta)}e^{i\alpha\rho\cos(\psi-\beta)}e^{\alpha R\sin\gamma}\,\mathrm{d}\beta\,\mathrm{d}\alpha$$

$$= \frac{i^n}{2\pi}e^{in\psi}\sum_{m=-\infty}^{\infty}\int_0^\infty \alpha^{p+1}J_m(\alpha R\cos\gamma)J_{m+n}(\alpha\rho)e^{\alpha R\sin\gamma}\,\mathrm{d}\alpha\, e^{-im(\varphi-\psi)} \tag{23}$$

[notice that $I_n(0)$ coincides with eqn (10)].

Just as above, components of the kernels of integral operators (15) are linear combinations of series $I_n(\gamma)$ replacing α_1, α_2 in the kernel-symbols (16), (17) in accordance with the rule indicated under eqn (9).

The key role in applying the Mellin transform to $I_n(\gamma)$ is played by the equality (Ditkin and Prudnikov, 1974)

$$\int_0^\infty J_m(aR)e^{-pR}R^{s-1}\,\mathrm{d}R = \Gamma(s+\nu)(p^2+a^2)^{-s/2}P_{s-1}^{-m}\left(\frac{p}{\sqrt{p^2+a^2}}\right), \tag{24}$$

$P_\nu^\mu(z)$ is the Legendre function.

It appears to yield the same representation of $M_s[I_n(\gamma)]$ and $M_s[zI_n(\gamma)]$ as eqn (11) but with

$$G_1(s,m,\gamma) = 2^{1-s}\Gamma(s+m)\begin{cases}P_{s-1}^{-m}(-\sin\gamma) & \text{for} \quad I_n\\ \sin\gamma P_s^{-m}(-\sin\gamma) & \text{for} \quad zI_n\end{cases}$$

instead of $G_1(s,m) = G_1(s,m,0)$.

Thus, from eqns (18) we arrive at the Mellin transforms $\mathbf{U}(s,\varphi,\gamma) = M_s[\mathbf{u}]$ and $\mathbf{T}(s+1,\varphi,\gamma) = M_{s+1}[\tau]$ also expressed as one-fold integrals over polar angles $\psi_j \in S_j$:

$$\mathbf{U}^i(s,\varphi,\gamma) = \sum_j \mathbf{P}_{ij}\int_0^{\theta_j}\mathbf{K}^{ij}(s,\varphi_j,\gamma_j,\psi_j)\mathbf{Q}_j(s+1,\psi_j)\,\mathrm{d}\psi_j,$$

$$\mathbf{T}^i(s+1,\varphi,\gamma) = \sum_j \mathbf{P}_{ij}\int_0^{\theta_j}\mathbf{T}^{ij}(s+1,\varphi_j,\gamma_j,\psi_j)\mathbf{Q}_j(s+1,\psi_j)\,\mathrm{d}\psi_j, \tag{25}$$

where $\varphi_j = \varphi_j(\varphi)$, $\gamma_j = \gamma_j(\varphi)$, θ_j are opening angles of the wedge-shaped sides S_j, and components of $\mathbf{K}^{ij}$, $\mathbf{T}^{ij}$ are performed as linear combinations of series $M_s[I_n(\gamma)]$, $M_s[zI_n(\gamma)]$.

Consequently, discretisation in terms of basis functions $v_k^j(\psi_j)$ given at the sides S_j:

$$\mathbf{Q}_j(s+1,\psi_j) = \sum_k \mathbf{t}_k^j(s)v_k^j(\psi_j)$$

leads with projectors $w_l^i(\varphi_l)$ to algebraic system (6) where $\mathbf{t}_k = \{\mathbf{t}_k^1,\ldots,\mathbf{t}_k^N\}$ (N is a number of sides S_j) and $\mathbf{a}_{lk}$ are block matrices $3N\times 3N$ composed of matrix-symbols $\mathbf{K}^{ij}$, $\mathbf{T}^{ij}$ of operators (25) with $\hat{I}_n$ replacing $M_s[I_n(\gamma)]$, $M_s[zI_n(\gamma)]$. Arrays of the constants $d_1^j(m,k)$ in the final series $\hat{I}_n$ remains as before in eqn (13) [index j in d_1^j means that this array relates to the side S_j, i.e. $\psi_j\in[0,\theta_j]$, $\bar{\psi}_j = (2\psi_j-\theta_j)/\theta_j$], but as for

$$d_2^{ij}(m,l)=\int_{-1}^{1} w_l^i(\varphi_i)G_1(s,m,\gamma_j(\varphi_i))e^{-im\varphi_j(\varphi_i)}\,\mathrm{d}\bar{\varphi}_i,\quad \bar{\varphi}_i=(2\varphi-\theta_i)/\theta_i \tag{26}$$

the difference is essential. First, since γ_j enters in G_1, the angle variables are not separated out from s, hence, d_2^{ij} are not constants relative to parameter s and must be recomputed at each step in the $\Delta(s)$ roots search. Second, when $i\neq j$, the co-ordinate angles φ_j, γ_j, locating the point $\mathbf{x}_j$ at the side of projection S_i in the co-ordinates connected with S_j, are functions of the variable $\varphi_i\in S_i$ (Fig. 4). The specific dependencies $\varphi_j=\varphi_j(\varphi_i)$, $\gamma_j=\gamma_j(\varphi_i)$ are determined by a mutual arrangement of the sides. They are quite expressible in terms of trigonometric functions.

In other respects the general scheme remains as before. Difficulties of d_2^{ij} computing are not so problematic as they might seem. Moreover, for a large m, they are effectively approximated by asymptotic expansions.

We would like to emphasise once again that, first, weight orders δ_1, δ_2 of basis functions eqn (14) depend on the angles between sides; they have to be chosen as the main orders of 2D stress behaviour at the tops of corresponding elastic wedges. And, second, simultaneously with orders of stress singularities $\gamma_k=s_k+1$, the method yields explicit angular stress distribution in the volume as $R\to 0$:

$$\tau^i(R,\varphi,\gamma)\sim\sum_k \mathbf{c}_k^i(\varphi,\gamma)R_k^{-\gamma}, \tag{27}$$

where, taking into account eqns (18), (25),

$$\mathbf{c}_k^i(\varphi,\gamma)=\sum_j \mathbf{P}_{ij}\int_0^{\theta_j}\mathbf{T}^{ij}(s_k+1,\varphi_j,\gamma_j,\psi_j)\,\mathrm{res}\,\mathbf{Q}_j(s+1,\psi_j)\,|_{s=s_k}\,\mathrm{d}\psi_j.$$

Below there are numerical examples illustrating the method with several contact and crack problems. To gain a better understanding of the practical implementation of the method, its application to the wedge-shaped crack is given with additional specific details.

3. Contact problems

3.1. *Wedge-shaped punch*

In the special case when the trihedron in Fig. 3 is rigid, it acts on the elastic base as a rigid punch. Only eqn (20), coinciding with eqn (1) with the kernel-symbol $\mathbf{K}(\alpha_1,\alpha_2,0)$ eqn (16) and $\mathbf{q}=\{\tau_{xz},\tau_{yz},\sigma_z\}$, remains to be dealt with in this case. With smooth contact the problem leads to the scalar integral equation relative to the normal contact stress component σ_z as the unknown q with $K(\alpha_1,\alpha_2)=-(1-\nu)/(\mu\alpha)$.

Dependence of the singular exponent γ on the angle opening 2θ in the scalar case was first computed by Rvachev and Procenko (1968) and Bazant (1974). In the general case of an adhering punch the first results were obtained asymptotically for a small θ by Parihar and Keer (1979) and, as the first realisation of the scheme described above, were computed by Babeshko et al. (1981) for

the total range $0 \leqslant \theta \leqslant \pi$ (Figs 5 and 6). The case of friction contact, including the moving punch, has been investigated in Babeshko et al. (1989) and Glushkov and Glushkova (1988). In addition to the orders γ_i, the plots of averaged factors $(1/2\theta)\int_{-\theta}^{\theta} c_i(\varphi)\,d\varphi$, obtained as the residuals at the poles, are given in the latter paper.

Values γ_i in Figs 5–6 are shown in the strip of singularity $0 \leqslant Re\,\gamma \leqslant 3/2$. The vertical dashed line in the figures shows an approximate limit of θ to which the asymptotic results of Parihar and Keer (1979) accord with the plotted curves. For the Poisson ratio $\nu = 0.5$, system eqn (20) falls into three independent scalar integral equations relative to contact stress components τ_{rz}, $\tau_{\varphi z}$, σ_z. Each equation yields a unique real value γ_i, $i = 1, 2, 3$. Since the curves $\gamma_i(\theta)$ are varied continuously with a gradual change of ν, in the figures each of them is marked conditionally as these stress components for $\nu \neq 0.5$ too. When $\nu \neq 0.5$, different real values γ_i for σ_z and τ_φ merge together and then split in two complex conjugate values $\gamma = a \pm ib$ at a mid range of θ. Since residuals $c(\varphi, z) = |c|e^{i\arg c}$ at those poles are also conjugate, each pair of the poles contributes in the contact stress field as the oscillate singularity $2|c|r^{-a}\cos(b\ln r - \arg c)$ as $r \to 0$. Sketches of the pole traces in the complex γ-plane are given in the right side of the figures. For $\nu = 0$ the orders of σ_z, τ_φ become the same and complex over the whole range $0 \leqslant \theta \leqslant \pi$.

3.2. *Elastic trihedron with one fixed side*

If, in contrast to the case just considered, the base is rigid and the trihedron is elastic, one has to reject eqn (20) and to deal with the system (19) in which $\mathbf{v}_1 = 0$. Among the six angles of the

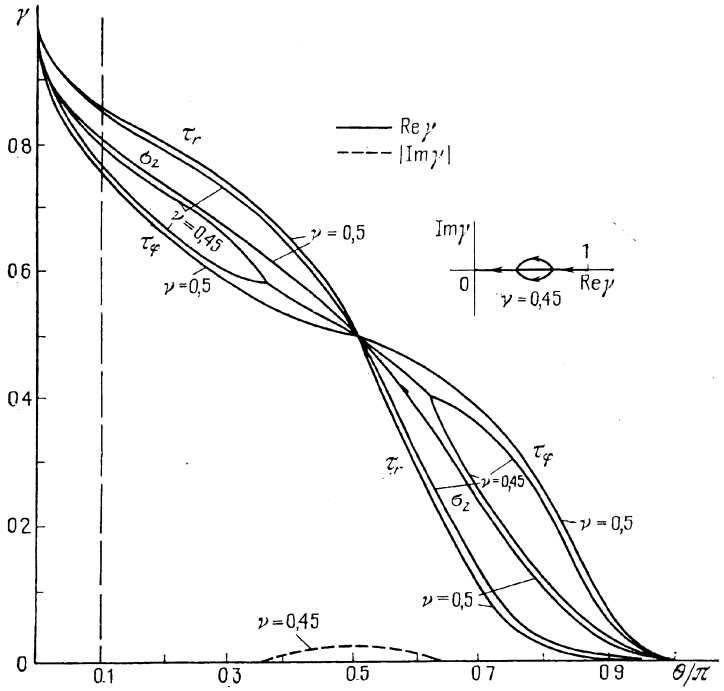

Fig. 5. Wedge-shaped punch bonded with a half-space. Singular exponents γ_i vs angle opening θ ($\nu = 0.5$ and 0.45).

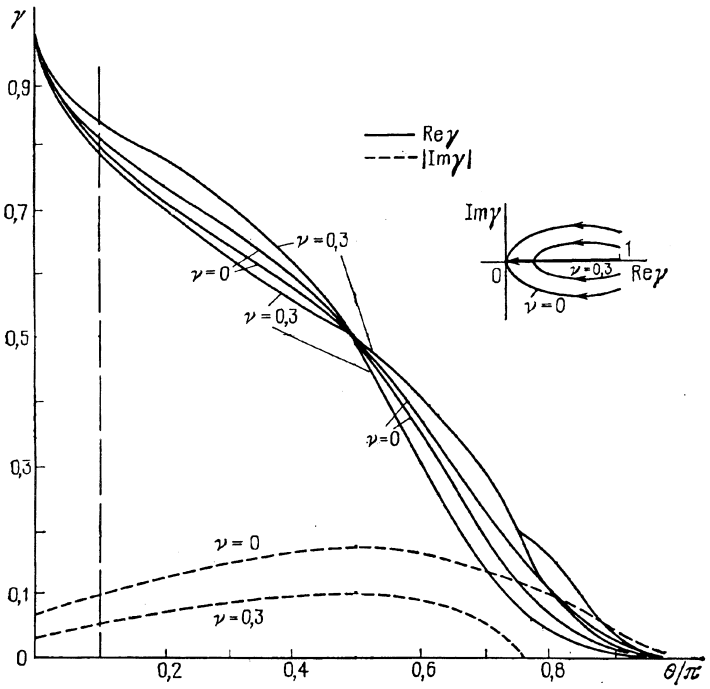

Fig. 6. The same as Fig. 5 ($v = 0.3$, $v = 0$).

trihedron (three opening angles θ_i of the sides S_i, and three angles $\pi-\beta_i$ between the sides S_i and S_{i+1}, $i = 1, 2, 3$; $(S_4 \equiv S_1)$), only three are required to set the geometry. Let these be θ_1 and $\beta_1 = \beta_3 = \beta$ (isosceles slopes) (Fig. 3). When $\theta_1 = \beta = \pi/2$ this is the top of a cube (point 5 in Fig. 1); if $\beta \to 0$, the trihedron is folded out in the half-space with a fixed surface sector just as in the previous wedge-shaped punch problem. Therefore, exponents γ_i for the punch were used as initial values for finding the orders of singularity of a trihedron by tracing them numerically in the complex plane by gradually varying the angles.

Thus, Figs 7 and 8 show the results of such varying from the quarter plane punch (the circles on the vertical axis) to the top of a cube: $\theta_1 = \pi/2$, $0 \leqslant \beta \leqslant \pi/2$ (Fig. 7), and further, from the trihedral corner to a dihedron (the quarter-space wedge) with free-fixed sides: $\beta = \pi/2, \pi/2 \leqslant \theta_1 \leqslant \pi$ (Fig. 8). Along with the "punch" exponents γ_i, $i = 1, 2, 3$ two additional orders γ_4, γ_5 emerging from $\gamma = 0$, $\beta = 0$ were found in the strip $0 \leqslant Re\ \gamma \leqslant 3/2$ by doing so. In addition to the punch case, we used as a control the results of Matveenko and Minakova (1988) and Thatcher (1992) for the top of the cube (the asterisk in Fig. 7) and the well-known 2D order $\gamma = 0.289$ for the elastic wedge (the black dot in Fig. 8). One can see in the figures the value of $Re\ \gamma_3$ correlates well with those results but the others seem to contradict them. The matter of these extra branches has not been investigated and explained properly yet, although the fact that their values in the ultimate case of the elastic wedge (Fig. 8, $\theta_1 = \pi$, branches 1, 2, 4) coincide with the orders 0.456, 0.333, 0.0915 for the free–free wedge with the supplementary angle opening $3\pi/2$ may serve as the hint of their nature. It looks as if they resulted artificially from the used superposition technique eqns

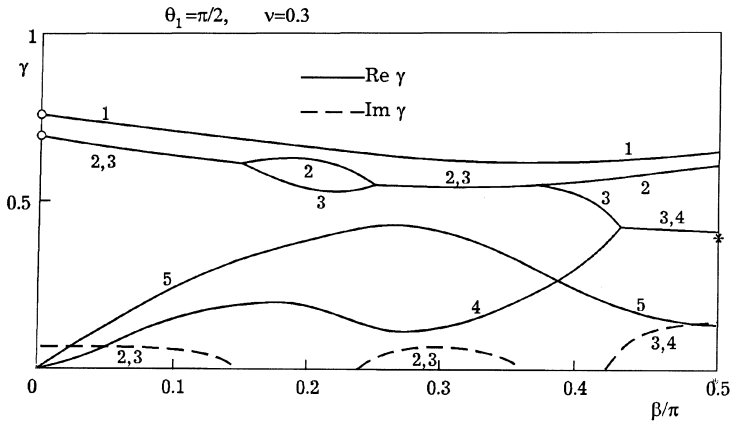

Fig. 7. Singularity orders at the trihedral vertex shown in Fig. 3 ($\theta_1 = \pi/2$, rigid base) vs β from the half-space subjected to the quarter-plane punch ($\beta = 0$) to the top of a cube ($\beta = \pi/2$). The asterisk marks the value obtained by Matveenko and Minakova, and by Thatcher.

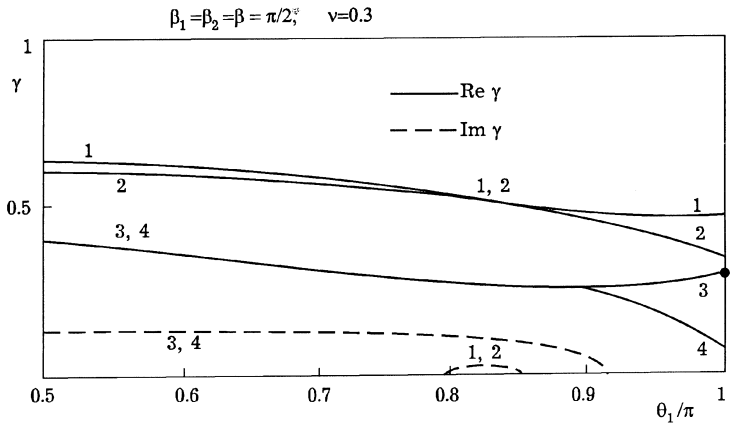

Fig. 8. The same as Fig. 7. Further unfolding from the cube top ($\beta = \pi/2$, $\theta_1 = \pi/2$) to the dihedral corner ($\theta_1 = \pi$). The black dot is the 2D singularity order.

(18)–(19) that yields the spectral points not only for the convex intersection of the half-spaces but for non-convex joins of the half-space pairs as well. Apparently, these extra poles, being found as the roots of denominator, are removed by zeros of the numerators, i.e. they are redundant for the final stress field at the top. The usual BIEs with respect to unknown stress and displacement vectors on the surface instead of the auxiliary functions $\mathbf{q}_j$ promise to be free from those redundant poles. To check this supposition this way has been trying now.

4. Crack problems

4.1. *Wedge-shaped crack*

Let us consider an elastic space $-\infty \leqslant x, y, z \leqslant \infty$ containing in the plane $z = 0$ a wedge-shaped crack Ω (infinitely thin slit with the stress-free sides, points 2 in Fig. 1) $-\theta \leqslant \varphi \leqslant \theta$, $0 \leqslant r \leqslant \infty$. The crack is subjected to a given exterior stress field $\mathbf{p}$ which causes the more field $\tau = \{\tau_{xz}, \tau_{yz}, \sigma_z\}$. The latter is expressed through the unknown crack opening displacement

$$\mathbf{v}(x, y) = \mathbf{u}^+(x, y, 0^+) - \mathbf{u}^-(x, y, 0^-), \quad (x, y) \in \Omega \tag{28}$$

as the following convolution integral

$$\tau(\mathbf{x}) = \int\int_{\Omega} \mathbf{k}_1(x-\xi, y-\eta, z)\mathbf{v}(\xi, \eta)\, \mathrm{d}\xi\, \mathrm{d}\eta. \tag{29}$$

Here, $\mathbf{u}^{\pm}$ are displacements for $z \geqslant 0$ and $z \leqslant 0$, respectively.

The unknown c.o.d. $\mathbf{v}$ is determined from the integral equation

$$\mathscr{K}_1\mathbf{v} \equiv \int\int_{\Omega} \mathbf{k}_1(x-\xi, y-\eta, 0)\mathbf{v}(\xi, \eta)\, \mathrm{d}\xi\, \mathrm{d}\eta = -\mathbf{p}(x, y, 0), \quad (x, y) \in \Omega \tag{30}$$

that follows from the stress-free conditions on the sides. The actual form of the kernel $\mathbf{k}_1$ is well-known; in the context of the offered technique it is derived easily starting from the Fourier transform solutions

$$\mathbf{u}^{\pm}(\mathbf{x}) = \mathscr{K}^{\pm}\mathbf{q} \equiv \frac{1}{2\pi}\int\int_{-\infty}^{\infty} \mathbf{K}^{\pm}(\alpha_1, \alpha_2, z)\mathbf{Q}(\alpha_1, \alpha_2)e^{-i(\alpha_1 x + \alpha_2 y)}\, \mathrm{d}\alpha_1\, \mathrm{d}\alpha_2 \tag{31}$$

for upper $z \geqslant 0$ ($\mathbf{u}^+$) and lower $z \leqslant 0$ ($\mathbf{u}^-$) half-spaces subjected to a surface loading $\mathbf{q}(x, y) = \tau(x, y, 0)$. Matrix $\mathbf{K}^-$ (Fourier transform of the half-space Green's matrix) is represented by eqn (16), $\mathbf{K}^+$ is derived from $\mathbf{K}^-$ by inverting the signs of the variable z and of the corresponding components of $\mathbf{q}$ and $\mathbf{u} = \{u_x, u_y, u_z\}$.

The Fourier transform of eqns (28) and of (29), (31) with $z = 0$ leads to equalities:

$$\begin{aligned} \mathbf{V}(\alpha_1, \alpha_2) &= \mathbf{U}^+(\alpha_1, \alpha_2, 0) - \mathbf{U}^-(\alpha_1, \alpha_2, 0) \\ \mathbf{Q}(\alpha_1, \alpha_2) &= \mathbf{K}_1(\alpha_1, \alpha_2, 0)\mathbf{V}(\alpha_1, \alpha_2) \\ \mathbf{U}^{\pm}((\alpha_1, \alpha_2, 0) &= \mathbf{K}^{\pm}(\alpha_1, \alpha_2, 0)\mathbf{Q}(\alpha_1, \alpha_2) \end{aligned} \tag{32}$$

from which it follows

$$\mathbf{K}_1(\alpha_1, \alpha_2, 0) = [\mathbf{K}^+(\alpha_1, \alpha_2, 0) - \mathbf{K}^-(\alpha_1, \alpha_2, 0)]^{-1}. \tag{33}$$

Namely, for the homogeneous case considered

$$\mathbf{K}_1(\alpha_1,\alpha_2,0)=\frac{\mu}{2(1-\nu)\alpha}\begin{pmatrix}\alpha^2-\nu\alpha_2^2 & \nu\alpha_1\alpha_2 & 0\\ \nu\alpha_1\alpha_2 & \alpha^2-\nu\alpha_1^2 & 0\\ 0 & 0 & \alpha^2\end{pmatrix}. \tag{34}$$

The kernel structure (34) shows that system (30) and, correspondingly, eqn (6), in fact, fall into independent equations relative to tangential v_x, v_y and normal v_z components of the unknown c.o.d. **v**. It should be noted, that representation eqn (33) is valid for an interface crack between dissimilar materials too, but the system is not split in that case. Nevertheless, the scheme of Section 2.1 is also quite applicable.

In line with the scheme, eqn (30) is brought by the Mellin transform to the equation [see eqn (4)]:

$$\int_{-\theta}^{\theta}\mathbf{K}_1(s,\varphi-\psi)\mathbf{V}(s-1,\psi)\,\mathrm{d}\psi=-\mathbf{P}(s,\varphi),\quad -\theta\leqslant\varphi\leqslant\theta \tag{35}$$

where

$$\mathbf{K}_1=\frac{\mu}{2(1-\nu)}\begin{pmatrix}\nu_0 I_0-\nu_4 I_2^+ & -i\nu_4 I_2^- & 0\\ -i\nu_4 I_2^- & \nu_0 I_0+\nu_4 I_2^+ & 0\\ 0 & 0 & I_0\end{pmatrix},$$

$$I_2^{\pm}=(I_2\pm I_{-2}),\quad \nu_0=1-\nu/2,\quad \nu_4=\nu/4, \tag{36}$$

I_n are series (11) without ρ^{s-p-2} entered in **V**; $p=1$.

Blocks $\mathbf{a}_{lk}$ of matrix **A** eqn (6) are matrices (36) with I_n replaced by $\hat{I}_n(l,k)$ eqn (12) with $v_k(\psi)=(1-\bar{\psi}^2)^{1/2}P_k^{(1/2,1/2)}(\bar{\psi})$, $w_l(\varphi)=P_l(\bar{\varphi})$. Like in the punch case above, there are three singular exponents γ_i found as roots of $\Delta(s)=\det\mathbf{A}$ in the strip of singularity. Notice that limits of this strip are determined by considering the stress τ behaviour near the crack tip, which connected here with the unknown **v** by relation (29) or in the Mellin transforms as

$$\mathbf{T}(s,\varphi,z)=\int_{-\theta}^{\theta}\mathbf{K}_1(s,\varphi-\psi,z)\mathbf{V}(s-1,\psi)\,\mathrm{d}\psi \tag{37}$$

(the kernel of eqn (35) $\mathbf{K}_1=\mathbf{K}_1(s,\varphi-\psi,z)\,|_{z=0}$).

Correspondingly,

$$\tau(r,\varphi,0)\sim\sum_{i=1}^{\infty}\mathbf{c}_i(\varphi,0)z^{-\gamma_i},\quad z\to 0,\quad \gamma_i\colon Re\,\gamma_i<3/2$$

$$\mathbf{c}_i=\int_{-\theta}^{\theta}\mathbf{K}_1(\gamma_i,\varphi-\psi,0)\,\mathrm{res}\,\mathbf{V}(s-1,\psi)\,|_{s=\gamma_i}\,\mathrm{d}\psi. \tag{38}$$

In distinction to the contact stress, all $\gamma_i(\theta)$ are real over the whole range θ. Since the structure of $\mathbf{K}_1$ eqn (34), poles of normal and tangential components of **V** contribute independently in σ_z and τ_{xz}, τ_{yz} in the crack plane $z=0$. (With $z\neq 0$ matrix K_1 is filled and each pole contributes in all

stress components.) This order of stress singularity of the normal component σ_z, obtained by Rvachev and Procenko, and Bazant, in fact, is the same as for the contact stress under the smoothly contacting punch, with angle opening $2(\pi-\theta)$ (the scalar integral eqn (30) with respect to v_z can be converted into the equation relative to σ_z with the same kernel symbol $K = c/\alpha$ as for the smooth punch). The order γ_3 is independent on the Poisson ratio v whereas "tangential" orders γ_1, γ_2 depend on both θ and v. Factors $\mathbf{c}_i$ for the normal stress component in the crack plane and "tangential" singular exponents for γ_1, γ_2 have been obtained in Glushkov and Glushkova (1992) (see also Fig. 9). With $v = 0$ the two different values γ_1, γ_2 in Fig. 9 merge together yielding the only curve $\gamma(\theta)$ coinciding with the "normal" order $\gamma_3(\theta)$.

It is worthy of note that in spite of extracting and summing explicitly the slow convergent components of the series based upon asymptotics as $\lambda = m\theta \to \infty$, it does not help when $\theta \to 0$ and λ is not large for very large values of m. As a consequence, the real applicability of the approach is limited from below by a certain value θ_0: $0 < \theta_0 < \theta \leqslant \pi$ depending on computational power only. The limitation is not too hindering for even with PC 386, the two-digit accuracy has been obtained for $\theta > 0.05\pi$. Nevertheless, the asymptotic methods like those developed by Parihar and Keer (1979) or by Movchan and Nazarov (1990) supplement numerical schemes very well, allowing, in particular, to control computation in the critical zones. Thus, we are thankful to Prof. S. A. Nazarov who has pointed out an incorrectness of the numerical results in the vicinity of $\theta = 0$ shown in our paper (Glushkov and Glushkova, 1992). The curves of Fig. 9 recomputed for a small θ with longer series are already in accord with asymptotics derived by Movchan and Nazarov:

$$\gamma_i(\theta) = g_i\theta^2/\pi^2 + O(\theta^3), \quad \theta \to 0, \quad i = 1, 2, 3$$

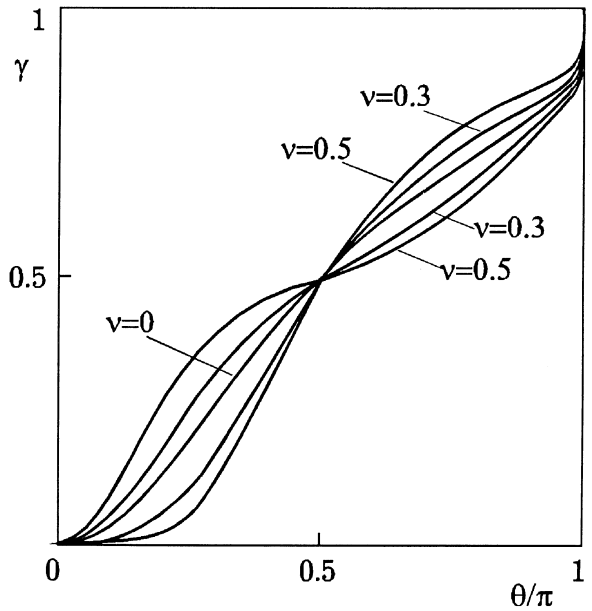

Fig. 9. Wedge-shaped crack. Singularity orders of the shear stress components τ_{xz}, τ_{yz} in the crack plane vs angle opening θ ($v = 0$, 0.3, 0.5).

$$\begin{cases} g_1 = (2\lambda^2+9\lambda\mu+5\mu^2)/(\lambda+2\mu)(\lambda+3\mu)(\lambda,\mu \text{ are the Lamé constants}) \\ g_2 = \mu/(\lambda+\mu) \\ g_3 = 1 \end{cases} \tag{39}$$

and

$$\gamma_i(\theta) = 1-1/2(\ln 2-\ln(1-\theta/\pi))+O(|\ln(1-\theta/\pi)|^{-2}), \quad \theta \to \pi. \tag{40}$$

4.2. *Surface-breaking crack*

If the crack front meets the surface of a sample (Fig. 1, points 4), the point of intersection is essentially a polyhedral non-convex corner. This problem (mainly the special case of the orthogonal to the surface crack front) was considered by Folias (1975), Benthem (1977), Bazant and Estenssoro (1979), Ghahremani (1991), Ghahremani and Shih (1992), and Leguillon (1995), among the others. Recent numerical results (Glushkov et al., 1998) for any slope angle θ between the front and the surface [however, in the orthogonal to the surface $z = 0$ crack plane $y = 0$ (Fig. 10)] are given below in Figs 11 and 12.

The system of BIEs for this non-convex volume may be derived in the framework of the offered general scheme by sewing BIEs like eqn (19) for the two right-angle trihedrons. However, with such a special case as a crack, essentially simpler integral equations are obtained basing upon the crack field representation eqn (29). Combination of the crack stress field τ of the form eqn (29) and of the field "reflected" from the surface $z = 0$ in the half-space leads to the following system:

$$\int\int_{\Omega} [\mathbf{k}_1(x-\xi, z-\zeta)+\mathbf{k}_2(x-\xi, z, \zeta)]\mathbf{v}(\xi,\zeta)\,\mathrm{d}\xi\,\mathrm{d}\zeta = -\mathbf{p}(x,0,z), \quad (x,z)\in\Omega. \tag{41}$$

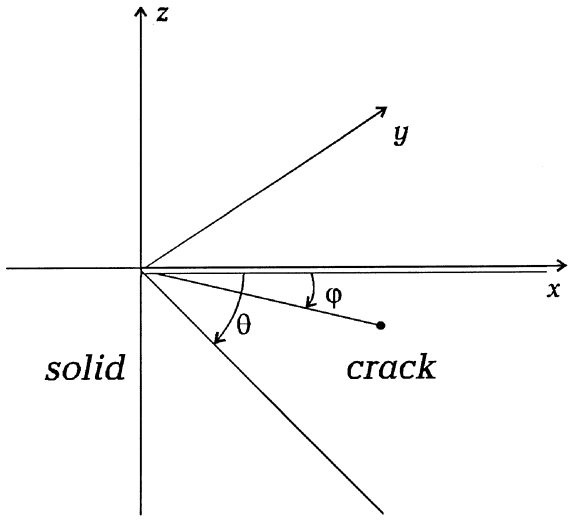

Fig. 10. Surface-breaking crack geometry.

Here, symbol of matrix $\mathbf{k}_1$ results from eqn (34) by changing the rows and columns in accordance with the new orientation of the crack plane $y = 0$ and co-ordinate axis re-designation ($z \to y$, etc.):

$$\mathbf{K}_1 = \frac{\mu}{2(1-\nu)\alpha}\begin{pmatrix} \alpha^2-\nu\alpha_2^2 & 0 & \nu\alpha_1\alpha_2 \\ 0 & \alpha^2 & 0 \\ \nu\alpha_1\alpha_2 & 0 & \alpha^2-\nu\alpha_1^2 \end{pmatrix},$$

and

$$\mathbf{k}_2 = \frac{1}{4\pi^2}\int_{-\infty}^{\infty}\int_{-\infty}^{\infty}\mathbf{K}_2(\alpha_2,\alpha_2,z,\zeta)e^{-i\alpha_1(x-\xi)+\alpha(z+\zeta)}\,\mathrm{d}\alpha_1\,\mathrm{d}\alpha_2$$

$$\mathbf{K}_2 = \frac{i\mu}{2(1-\nu)}\begin{pmatrix} (1,1) & 0 & (1,3) \\ 0 & (2,2) & 0 \\ (3,1) & 0 & (3,3) \end{pmatrix}$$

$$(1,1) = i\{(1-\nu)(\alpha_1^4+\alpha_2^4)/\alpha+(3-4\nu)(1-2\nu)\alpha_1^2\alpha_2^2/\alpha+(3-4\nu)z\alpha_1^2\alpha_2^2 + \zeta[(3-4\nu)\alpha_1^2\alpha_2^2+2\alpha\alpha_1^2\alpha_2^2 z]\}/\alpha^2$$

$$(1,3) = \alpha_1\{(1-\nu)+\alpha_2^2 z/\alpha+\zeta[(3-4\nu)\alpha_2^2/\alpha+2\alpha_2^2 z]\}$$

$$(3,1) = -\alpha_1\{(1-\nu)+\alpha_2^2(3-4\nu)z/\alpha+\zeta[\alpha_2^2/\alpha+2\alpha_2^2 z]\}$$

$$(3,3) = i\{(\nu\alpha_2^2+(1-\nu)\alpha^2)/\alpha+\alpha_2^2 z+\zeta[\alpha_2^2(1+2\alpha z)]\}$$

$$(2,2) = i\{4(-4\nu^2+2\nu+1)\alpha_2^2+(1-8\nu+8\nu^2)\alpha_2^4/\alpha^2+8\nu^2\alpha^2 + [4\nu+(3-4\nu)\alpha_2^2/\alpha^2]\alpha_2^2\alpha z+\zeta[(4\nu+(3-4\nu)\alpha_2^2/\alpha^2)\alpha_2^2\alpha+2\alpha_2^4 z]\}/\alpha.$$

As before (Section 4.1), eqn (41) follows from the stress-free conditions on the crack sides $y = 0$, $(x, z) \in \Omega$ and actually is split into normal and tangential components too.

After the Mellin transformation in the polar co-ordinates

$$\begin{cases} x = r\cos\varphi \\ z = r\sin\varphi \\ r = \sqrt{x^2+z^2} \end{cases} \quad \begin{cases} \xi = \rho\cos\psi \\ \zeta = \rho\sin\psi \\ \rho = \sqrt{\xi^2+\zeta^2} \end{cases} \quad -\theta \leqslant \varphi, \quad \psi \leqslant 0$$

eqn (41) takes the form

$$\int_{-\theta}^{0}[\mathbf{K}_1(s,\varphi-\psi)+\mathbf{K}_2(s,\varphi,\psi)]\mathbf{V}(s-1,\psi)\,\mathrm{d}\psi = -\mathbf{P}(s,\varphi), \quad -\theta \leqslant \varphi \leqslant 0. \tag{42}$$

Components of the kernel $\mathbf{k}_2$ in this situation are expressed in terms of series

$$E_n = \frac{1}{4\pi^2}\int_0^{\infty}\alpha^2 e^{\alpha(z+\zeta)}\int_0^{2\pi}e^{-i\alpha_1(z-\xi)}e^{in\beta}\,\mathrm{d}\beta\,\mathrm{d}\alpha$$

$$= \frac{i^n}{2\pi}\int_0^\infty \alpha^2 e^{\alpha(z+\zeta)} \sum_{m=-\infty}^{\infty} J_m(\alpha r\cos\varphi)J_{m+n}(\alpha\rho\cos\psi)\,\mathrm{d}\alpha.$$

Hence, the components of $\mathbf{K}_2$ also are series like I_n, but, by according equality (24), with the Legendre functions $P_{\mu_1}^{-m}(-\sin\varphi)P_{\mu_2}^{-m}(-\sin\psi)$ ($\mu_1 = s-1$ or s, $\mu_2 = 2-s$ or $3-s$) instead of the oscillate exponents $e^{-im(\varphi-\psi)}$. The detailed specific representation of the final series and the matrix $\mathbf{A}(s)$ of eqn (6) is given in Glushkov et al., 1998.

Along similar lines as in Section 4.1 the stress behaviour as $R \to 0$ is expressed in terms of residuals at the poles s_i of $\mathbf{V}(s-1,\psi)$. In particular, for the stress field in the crack plane $y = 0$ we, reasoning from eqn (42), arrive at the expression

$$\tau(r,\varphi,0) \sim \sum_{i=1}^{\infty} \mathbf{c}_i(\varphi) r^{-\gamma_i}, \quad r \to 0, \quad -\pi < \varphi < -\theta \tag{43}$$

where

$$\mathbf{c}_i(\varphi) = \int_{-\theta}^{0} [\mathbf{K}_1(s_i, \varphi-\psi) + \mathbf{K}_2(s_i,\varphi,\psi)]\,\mathrm{res}\,\mathbf{V}(s-1,\psi)\,|_{s=s_i}\,\mathrm{d}\psi, \quad \gamma_i = s_i.$$

The chief surprise encountered in the course of eqn (42) discretisation was in the choice of the constants δ_1, δ_2 for the weight function of the basis $v_k(\bar{\psi})$, $\psi = \theta(\bar{\psi}-1)/2$ [see eqn (14)]. While the c.o.d. behaviour at the crack front $\psi = -\theta$ ($\bar{\psi} = -1$) is the well-known square-root decrease resulting in $\delta_2 = 1/2$, its behaviour at the surface $z = 0$ ($\psi = 0$, $\bar{\psi} = 1$) depends on the mutual displacement of the crack side edges. At first glance it may appear to be arbitrary, i.e. $\mathbf{V}(s-1,\psi) \sim O(1)$ as $\psi \to 0$ and, hence, $\delta_1 = 0$. However, while $\delta_1 = 0$ was quite acceptable for the tangential case, we could not get any stable numerical results for the normal component with $\delta_1 = 0$ but only with $\delta_1 = 1$ (the latter was the next permissible value from the viewpoint of the series convergence after $\delta_1 = 0$). By this is meant that the singular term caused by the pole of the normal component V_y is accompanied by the displacement eigenform with the closed upper edges $0 \leqslant x < \infty$, $y = 0^{\pm}$, $z = 0$.

In the final analysis the orders $\gamma_i(\theta)$ has been obtained as zeros s_i of the truncated infinite matrices for the normal (Fig. 11) and tangential (Fig. 12) cases. Figure 11 gives dependencies on the slope θ for the first singular exponent γ_1 and the next non-singular γ_2 of σ_y (in the crack plane $y = 0$) obtained with truncated systems of size $N = 5$ for the Poisson ratios $\nu = 0$, 0.3, 0.4, 0.49, 0.5 (curves 1–5, respectively). As the chief difference from the cases considered above, the curve $\gamma_1(\theta)$ goes off the strip $0 \leqslant Re\,\gamma \leqslant 1$ and at a certain slope angle θ^* reaches the border of permissibility $Re\,\gamma = 1.5$. At this point the root γ_1 meets another root coming from above $Re\,\gamma > 1.5$ and becomes multiple. In accordance with the residual technique such a multiple pole contributes to the stress field an inadmissible term with a logarithmic factor $r^{-1.5}\ln r$ (if it is not eliminable, of course). In the range $\theta > \theta^*$ this multiple pole is split again into two complex conjugate values $\gamma = 1.5 \pm ib$ to which an acceptable oscillate term with factor $r^{-1.5}\cos(b\ln r - \arg c)$ corresponds in expansion (43).

One more interesting fact is that all curves γ_1 intersect when $\theta = 2\pi/3$, which means the singularity order $\gamma_1 = 0.59$ at this angle does not depend on the elastic properties.

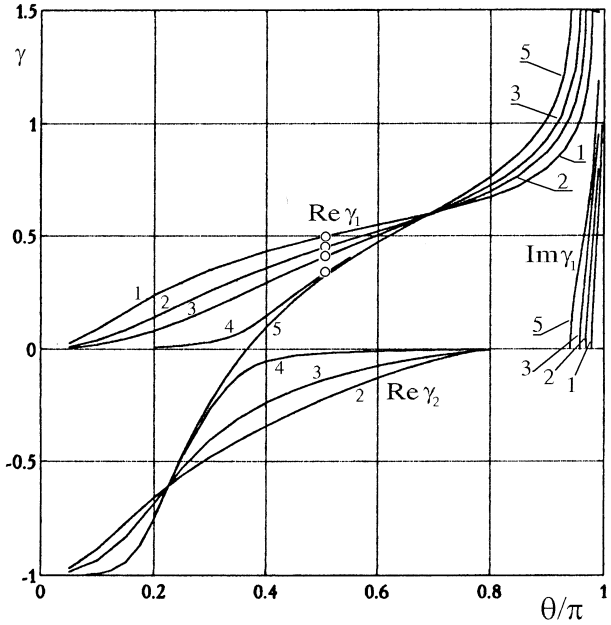

Fig. 11. Orders γ_1, γ_2 at the vertex of a surface-breaking crack vs slope θ. Normal stress component σ_y in the crack plane, $\nu = 0$, 0.3, 0.4, 0.49, 0.5 (curves 1–5, respectively).

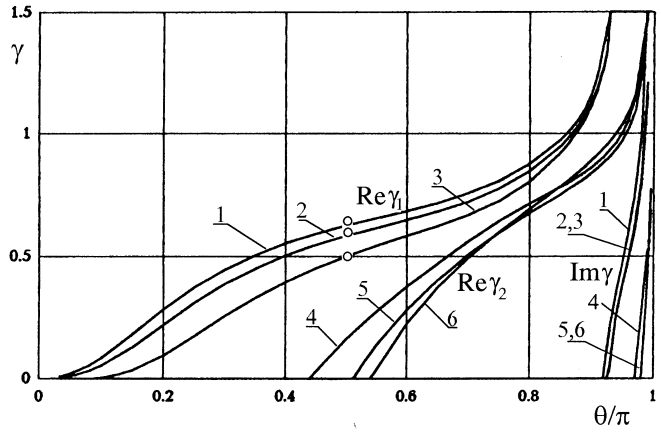

Fig. 12. The same for the shear stress components in the crack plane, $\nu = 0.5$, 0.3, 0; γ_1 (curves 1–3), γ_2 (4–5).

Similar to the wedge-shaped crack, $\gamma_1 \to 0$ as $\theta \to 0$ being held against the axis $\gamma = 0$ with $\nu \to 0.5$, while $\gamma_2 \to 0$ as $\theta \to \pi$, also approaching the axis from below, and both merge completely at $\nu = 0.5$. Since the pole $\gamma = 0$ is eliminable, the sole exponent at $\nu = 0.5$ is combined from the remaining parts of γ_1 and γ_2 in the strip $-1 < Re\,\gamma \leqslant 1.5$.

As for the tangential case (shear components τ_{xy}, τ_{yz} in the crack plane), the second exponent γ_2 also becomes singular for θ greater than about $\pi/2$ (Fig. 12). Here curves 1–3 relate to γ_1 and 4–6

to γ_2 for $v = 0.5$, 0.3, 0, respectively. The circles in Figs 11 and 12 mark the exponents for the orthogonal crack front $\theta = \pi/2$ given in Ghahremany (1991) that were used as a control.

5. Conclusion

We have demonstrated the applicability of the Melling transform approach for extracting out singular components of a solution near an arbitrary polyhedral vertex. There are not any insuperable difficulties in extending this method for anisotropic media or multi-material joints. The method's strength is low computational expense, but it demands heavy priori analytical calculations. As a worthy tribute, these efforts yield not only effective code but also a semi-analytical explicit representation of the eigenmodes, paving the way to creating so-called 3-D singular elements, that, being implemented in the FEM schemes, might be of great use in failure analysis of complex-structured critical zones.

Acknowledgements

The authors are grateful to Prof. V. A. Babeshko for initiating this research and suggesting the main idea of the method. Various aspects of this work were discussed fruitfully with Profs V. M. Alexandrov, S. A. Nazarov, Drs D. Leguillon, E. I. Shifrin. We are also thankful to Dr M. Hemesath for improving the English of this paper. The work was supported in part by the International Science Foundation (Soros' Foundation) Grant No. J5P100, 1995; and by the Russian Foundation for Basic Research Grants No. 95-01-00266 and No. 97-01-00429.

References

Abdei-Messiei, Y. S. and Thatcher, R. W. (1990) Estimating the form of some three-dimensional singularities. *Commun. Appl. Numer. Meth.* **6,** 333–341.

Babeshko, V. A., Glushkov, E. V. and Glushkova, N. V. (1981) Singularities at corners of three-dimensional stamps in contact problems. *Sov. Phys. Dokl.* **26**(3), 290–292.

Babeshko, V. A., Glushkov, E. V. and Zinchenko, J. F. (1989) *Dynamics of the Inhomogeneous Linear-Elastic Media.* Nauka, Moscow, p. 344 (in Russian).

Babeshko, V. A., Glushkov, E. V., Glushkova, N. V. and Lapina, O. N. (1991) Anomalies of stresses in the neighborhood of the vertex of an elastic trihedron. *Sov. Phys. Dokl.* **36**(6), 445–447.

Bateman, H. and Erdélyi, A. (1953) Higher transcendental functions, v. 2.

Bazant, Z. J. (1974) Three-dimensional harmonic functions near termination or intersection of gradient singularity lines: a general numerical method. *International Journal of Engineering Science* **12**(3), 221–243.

Bazant, Z. J. and Estenssoro, L. F. (1979) Surface singularity and crack propagation. *International Journal of Solids and Structures* **15,** 405–426.

Becker, I. and Schnark, E. (1990) Numerical calculation of singularities at re-entrant edges and corners for three dimensional crack problems. *Z. angew. Math. und Mech.* **70**(11), 529–530.

Benthem, J. P. (1977) State of stress at the vertex of a quarter-infinite crack in a half-space. *International Journal of Solids and Structures* **13,** 479–492.

Bogy, D. B. (1968) Edge-bonded dissimilar orthogonal elastic wedges under normal and shearing loading. *J. Appl. Mech.* **35,** 460–466.

Ditkin, V. A. and Prudnikov, A. P. (1974) *Integral Transformations and Operational Calculus*. Nauka, Moscow, p. 544 (in Russian).

England, A. H. (1971) On stress singularities in linear elasticity. *International Journal of Engineering Science* **9,** 571–585.

Folias, E. S. (1975) On the three-dimensional theory of cracked plates. *Trans. ASME J. Appl. Mech*. September, 663–674.

Ghahremani, F. (1991) A numerical variational method for extracting 3-D singularities. *International Journal of Solids and Structures* **27**(11), 1371–1386.

Ghahremani, F. and Shih, C. F. (1992) Corner singularities of three-dimensional planar interface cracks. *Trans. ASME J. Appl. Mech*. **59**(1), 61–68.

Glushkov, E. V. and Glushkova, N. V. (1988) *Stress Concentration Near the Corner Point of a Wedge-Shaped Moving Punch*. Kuban State University, Krasnodar. Manuscript deposited to VINITI No. 7745 B-88, 25 p. (in Russian).

Glushkov, E. V. and Glushkova, N. V. (1992) On stress singularities at a tip of 3-dimensional wedge-shaped crack. *Izvestiya Akademii Nauk SSSR. Mekhanika Tverdogo Tela*, No. 4, 82–86 (in Russian).

Glushkov, E. V., Glushkova, N. V. and Lapina, O. N. (1998) Orders of elastic stress singularity at a crack-surface intersection point (to appear in *Izvestiya RAN*, *Mekhanika Tverdogo Tela*) (in Russian).

Karp, S. N. and Karal, F. C. J. (1962) The elastic field behaviour in the neighbourhood of a crack of arbitrary angle. *Commun. Pure Appl. Math*. **15,** 413–421.

Kondrat'ev, V. A. (1968) Boundary problems for elliptic equations with conical or angular points. *Trans. Moscow Math. Soc*. **17,** 209–292.

Lapina, O. N. (1992) Stress singularity at polyhedral corner points. Kand. Sc. thesis, Kuban State University, Krasnodar, 65 p. (in Russian).

Leguillon, D. (1995) Computation of 3-D-singularities in elasticity. In *Boundary Value Problems and Integral Equations in Nonsmooth Domains*, ed. M. Costabel, M. Dauge and S. Nicaise. Lecture notes in pure and applied mathematics, Vol. 167, pp. 161–170. Marcel Dekker Inc., New York.

Matveenko, V. P. and Minakova, S. G. (1988) Numerical analysis of the stress singularity at a top of trihedral elastic corner. In *Mech. and Appl. Math.*: *All-Union Conference*: *Contemporary Problems of Informatic*, *Computating Technique and Automatization*. (Abstracts), Tula, pp. 38–42 (in Russian).

Movchan, N. V. and Nazarov, S. A. (1990) Asymptotics of the orders of singularity for the wedge-shaped cracks. *Bulletin of Leningrad State University Series* 1, iss. **3,** 34–38 (in Russian).

Parihar, K. S. and Keer, L. M. (1979) The singularity at the apex of a boundary wedge-shaped stamp. *J. Appl. Mech*. **46**.

Rvachev, V. L. and Procenko, V. S. (1977) Contact problems of elasticity for the non-classical areas. Naukova Dumka, Kiev (in Russian).

Schwartz, L. (1950–1951). *Theorie des Distributions*, I–II, Paris.

Taylor, M. E. (1981) *Pseudodifferential Operators*. Princeton, New Jersey.

Thatcher, R. W. (1995) Estimating the form of an elastic vertex singularity with mixed boundary conditions. In *Boundary Value Problems and Integral Equations in Nonsmooth Domains*: Proceedings of the Conference at the CIRM, Luminy, eds. M. Costabel, M. Dange, S. Nicaise. Marcel Dekker Inc., New york, pp. 285–298.

Theocaris, P. S. (1974) The order of singularity at a multi-wedge corner of a composite plate. *International Journal of Engineering Science* **12,** 107–120.

Williams, M. L. (1952) Stress singularities resulting from various boundary conditions in angular corner plates in extension. *J. Appl. Mech. ASME* **19,** 526–528.